Overexpression of miR-424-5p reduces cisplatin resistance by downregulating SMURF1 in gastric cancer

DAOHAN WANG, HE CUI, YONGJIA YAN, WEIHUA FU and LI LU

Department of General Surgery, Tianjin Medical University General Hospital, Tianjin 300052, P.R. China

Received July 4, 2024; Accepted November 22, 2024

DOI: 10.3892/ol.2025.14889

Abstract. Chemoresistance is a major obstacle in the treatment of gastric cancer (GC). Notably, aberrant expression of microRNAs (miRs) is closely related to tumor development and progression. In the present study, the role of miR-424-5p in the chemoresistance of GC was investigated. Reverse transcription-quantitative PCR was used to detect the expression levels of miR-424-5p in tissues and different cell lines. Cell viability and apoptosis were detected via a Cell Counting Kit-8 assay, western blotting and flow cytometry. The targeting relationship between miR-424-5p and SMAD-specific E3 ubiquitin protein ligase 1 (SMURF1) was verified via dual-luciferase reporter assays and the molecular mechanism was investigated by western blotting. The results revealed that miR-424-5p was expressed at low levels in GC tissues and cell lines, and that low miR-424-5p expression was associated with poor N stage and worse prognosis, especially in patients who received adjuvant chemotherapy. Further experiments revealed that the overexpression of miR-424-5p reduced cisplatin (CDDP) resistance and promoted GC cell apoptosis, whereas inhibiting miR-424-5p had the opposite effect. Mechanistically, it was found that miR-424-5p downregulated the expression of SMURF1 to regulate the expression of ING2 and p53, thereby modulating CDDP resistance in GC. In summary, the present study demonstrated that miR-424-5p may serve an important regulatory role in CDDP resistance in GC, and could be a potential diagnostic biomarker and therapeutic target for GC chemoresistance.

Correspondence to: Dr Weihua Fu or Dr Li Lu, Department of General Surgery, Tianjin Medical University General Hospital, 154 Anshan Road, Heping, Tianjin 300052, P.R. China
E-mail: tjmughgs_fwh@163.com
E-mail: luli_1989@126.com

Key words: microRNA 424-5p, gastric cancer, SMAD-specific E3 ubiquitin protein ligase 1, cisplatin, chemoresistance

Introduction

Gastric cancer (GC) is one of the most common malignancies, ranking as the fifth most common type of cancer globally, with ~1,089,103 new diagnoses each year. GC is also the fourth leading cause of cancer-related deaths and is responsible for 768,793 fatalities worldwide (1), and chemotherapy and radical surgery both serve important roles in standard treatment. Despite the recent availability of additional chemotherapy regimens, the combination of 5-fluorouracil and cisplatin (CDDP) is still the most commonly used chemotherapy regimen (2); however, resistance to chemotherapy may occur, leading to treatment failure and GC recurrence (3). Therefore, it is essential to investigate the mechanisms of drug resistance in stomach neoplasms to formulate a treatment strategy.

MicroRNAs (miRNAs/miRs) are an important group of noncoding RNA molecules that are characterized by short nucleotide sequences (20-24 nt), and are involved in the post-transcriptional regulation of gene expression in multicellular organisms by affecting both the stability and translation of mRNAs (4). Studies have shown that miRNAs are often involved in regulating tumor development as either tumor suppressors or promoters (5,6). It has also been reported that exogenous miRNA mimics regulate mRNA expression *in vivo* to achieve effective cancer treatment (7-9). miR-424-5p has been reported to be associated with the development of breast, bladder and colorectal cancer, may be a prognostic biomarker in melanoma, and may serve an anticancer role by inhibiting the proliferation of cervical cancer cells (10). However, miR-424-5p has not been well studied in GC. Our previous analysis of the Gene Expression Omnibus (GEO) database revealed that miR-424-5p may be a tumor suppressor and be associated with CDDP resistance (11).

The ubiquitin-proteasome system is an important method of protein degradation and E3 ubiquitination ligases are vital to this process. Inhibition of the ubiquitin-proteasome system may represent a new strategy to overcome chemotherapy resistance (12). SMAD-specific E3 ubiquitin protein ligase 1 (SMURF1), a member of the NEDD4 family, is a HECT-type E3 ubiquitin ligase that has an oncogenic role in various types of cancer, such as colon cancer and pancreatic ductal adenocarcinoma, through mediating ubiquitination (13).

Our previous study revealed that SMURF1 may be a target gene of miR-424-5p (11) and Nie *et al* (14) reported that the HECT-type ubiquitin ligase SMURF1 could target the tumor

suppressor ING2 for ubiquitination and proteasome-dependent degradation, further influencing the effect of ING2 on p53 activity, and suggested that SMURF1 may be involved in CDDP resistance. High SMURF1 expression is often associated with increased malignancy and poor prognosis in cancer (11,13). A growing body of evidence has verified that SMURF1 promotes tumor proliferation, migration and invasion both *in vitro* and *in vivo* (15). With further research, its role in drug resistance in tumors is gradually being investigated (16,17).

In the present study, the effects of miR-424-5p on SMURF1 expression in GC cells and its molecular role in regulating chemotherapeutic sensitivity were investigated. The present study aimed to gain a deeper insight into the molecular mechanisms underlying CDDP resistance in GC and to provide more information on targeted therapy for patients with GC.

Materials and methods

Tissue samples. Tumor tissues and adjacent tissues were collected from 80 patients who underwent radical gastrectomy for GC at Tianjin Medical University General Hospital (Tianjin, China). The tissues were stored in liquid nitrogen for RNA extraction and were fixed in 4% formalin at room temperature for 24 h and embedded in paraffin for immunohistochemistry (IHC). Median patient age was 67 years (range, 39-85 years). The histopathological diagnosis and grading were performed by two experienced pathologists, and clinicopathological characteristics were recorded. Survival data, such as overall survival (OS) and recurrence-free survival (RFS), were also collected to perform survival analysis via the Kaplan-Meier method and values were compared using the log-rank test (18). Written informed consent was obtained from all patients or their relatives for specimen collection. Ethics approval for this project was granted by the Investigation and Ethics Committee of Tianjin Medical University General Hospital (approval no. IRB2020-KY-640).

GC cell lines. The human GC cell lines NCI-N87 (cat. no. CL-0169) and MKN45 (cat. no. CL-0292), and the noncancerous gastric epithelial cell line GES-1 (cat no. AY09234) were obtained from the Laboratory of General Surgery, Tianjin Medical University General Hospital which purchased them from Procell Life Science & Technology Co., Ltd. (NCI-N87 and MKN45) and Ai-yan Biotechnology Co. Ltd. (GES-1). The human GC cell lines HGC27 (cat. no. CL-0107) and AGS (cat. no. CL-0022) were provided by Procell Life Science & Technology Co., Ltd. Short tandem repeat analysis was performed on these human cell lines for authentication. The GES-1, NCI-N87, MKN45 and HGC27 cells were cultured in RPMI-1640 (cat no. 11875093), whereas AGS cells were cultured in F12 (cat no. 11765054) supplemented with 10% fetal bovine serum (cat no. A5670701) and 1% penicillin/streptomycin (cat no. 15140122) (all from Gibco; Thermo Fisher Scientific, Inc.) at 37˚C in a humidified atmosphere with 5% CO_2.

Reverse transcription-quantitative (RT-q) PCR. Total RNA was extracted using RNA Isolater Total RNA Extraction Reagent (cat no. R401; Vazyme Biotech Co., Ltd.), and was converted to cDNA with the HiScript® III 1st Strand cDNA Synthesis Kit (cat no. R312; Vazyme Biotech Co., Ltd.) or the miRcute Plus miRNA First-Strand cDNA Kit (cat no. KR211; Tiangen Biotech Co., Ltd.), according to manufacturers' protocols. qPCR was performed using ChamQ Universal SYBR RT-qPCR Master Mix (cat no. Q711; Vazyme Biotech Co., Ltd.) or the miRcute Plus miRNA RT-qPCR Kit (cat no. FP411; Tiangen Biotech Co., Ltd.) according to the manufacturer's protocol. For the detection of miRNA, the qPCR cycling conditions were as follows: Initial denaturation step at 95˚C for 15 min, followed by 45 cycles at 94˚C for 20 sec (denaturation) and 60˚C for 34 sec (annealing and extension), concluding with a melting curve analysis. For mRNA detection, the qPCR cycling conditions included an initial denaturation step at 95˚C for 30 sec, followed by 40 cycles at 95˚C for 20 sec (denaturation) and 60˚C for 30 sec (annealing and extension), also concluding with a melting curve analysis. The reverse primers for miRNA were provided in the qPCR kit. The copy number of miR-424-5p in patient tissues was calculated via absolute quantification methods (19), and relative quantification was performed to evaluate the expression of miRNAs and mRNAs in cell lines, which was analyzed using the comparative $2^{-\Delta\Delta Cq}$ method (20). The amplification curve and standard curve of miR-424-5p are shown in Fig. S1. The primer sequences are shown in Table SI, and GAPDH and U6 were used as housekeeping genes for mRNA and miRNA expression, respectively. All procedures were performed in triplicate.

Vector construction and cell transfection. The miR-424-5p mimics and inhibitor, and the negative controls (ncs) were constructed by Shanghai GenePharma Co., Ltd. HGC27 and AGS cells were transfected in 6-well plates with the miR-424-5p inhibitor, mimics or ncs (50 pmol/ml) using Lipofectamine® 2000 (cat no. 11668019; Invitrogen; Thermo Fisher Scientific, Inc.) once they reached 30-50% confluence, following the manufacturer's instructions, at 37˚C in CO_2 for 24 h. After 24 h, the cells were harvested for subsequent experiments. The lentivirus used to knock down SMURF1 [short hairpin (sh)SMURF1] and its negative control (sh-nc; cat. no. 20221126) was constructed using the pCDH-CMV-MCS-EF1-copGFP-T2A-Puro vector (Shanghai GenePharma Co., Ltd.) as a backbone, whereas the SMURF1 overexpression lentivirus (LV-SMURF1) and its negative control (LV-nc) were constructed using the pLKO.1-copGFP-2A-PURO vector (Shanghai GenePharma Co., Ltd.). All lentiviral constructs were produced by Shanghai GenePharma Co., Ltd. using the 3rd generation system. The AGS and HGC27 cells were then infected with lentiviral particles (MOI=10) with the addition of 5 μg/ml polybrene (cat no. H8761; Beijing Solarbio Science & Technology Co., Ltd) for 8 h at 37˚C in a humidified atmosphere containing 5% CO_2. The culture solution was fully replaced at 24 h. The stable cell lines were selected with puromycin (cat. no. HY-B1743; MedChemExpress) after 3 days. RT-qPCR and western blotting were used to determine the transfection and infection efficiencies. All of the aforementioned sequences are presented in Table SII.

Colony formation assay. HGC27 and AGS cells transfected with miR-424-5p inhibitors, mimics or ncs were seeded into 6-well plates at a density of 1,000 cells/well, and were cultured

at 37˚C in a humidified atmosphere containing 5% CO_2, with the culture media replaced every 3 days. Colony formation was assessed after culturing the cells for 14 days. After washing the cells three times with phosphate-buffered saline, the colonies were fixed with 4% paraformaldehyde for 20 min and stained with 0.1% crystal violet (cat no. G1063; Beijing Solarbio Science & Technology Co., Ltd.) staining solution for 5 min at room temperature. Formations with >50 cells were identified as colonies under a dissecting microscope.

Wound healing assay. Cells were seeded into 6-well plates at a density of $2x10^5$ cells/well and were allowed to attach until they reached 80-90% confluence at 37˚C in a humidified atmosphere with 5% CO_2. Subsequently, a straight scratch was made using a 20-μl pipette tip in the cell monolayer, and cell migration was monitored and documented every 24 h under an inverted fluorescence microscope. The migration of the cells was calculated by measuring the distance covered by the cells at each time point via ImageJ 1.54g (National Institutes of Health). The cells were serum starved for 12 h prior to the migration assay to negate the effect of cell proliferation before migration, and then cultured with fresh medium containing 1% fetal calf serum.

Transwell and invasion assays. Cells ($5x10^4$/well) were seeded into the upper chambers of a 24-well Corning® 6.5 mm Transwell® with 5.0 μm Pore Polycarbonate Membrane Insert (cat. no. 3421; Corning, Inc.) to detect cell migration and invasion. To assess cell invasion, the insert was pre-coated with Matrigel (cat no. 354248; BD Biosciences) at 37˚C for 1 h. In addition, medium containing 10% fetal bovine serum was added to the lower chambers. After incubation for 24 h at 37˚C in a humidified atmosphere containing 5% CO_2, the migratory and invasive cells were stained with 0.1% crystal violet at room temperature for 30 min, and images were captured under an inverted fluorescence microscope. All assays were repeated at least three times.

Western blotting. Total protein was isolated from cells using RIPA buffer (cat no. R0010; Beijing Solarbio Science & Technology Co., Ltd.) supplemented with protease inhibitor (cat no. A32955; Thermo Fisher Scientific, Inc.). After the protein concentration was measured using the BCA assay, the protein samples were boiled and ~15 μg protein was separated by SDS-PAGE on 10% gels and transferred to PVDF membranes. After blocking non-specific binding sites with 5% non-fat dry milk (cat. no. D8340; Beijing Solarbio Science & Technology Co., Ltd.) at room temperature for 1 h. The membranes were probed with antibodies against SMURF1 (1:1,000; cat. no. 2174; Cell Signaling Technology, Inc.), caspase 3 (1:1,000; cat. no. 9662; Cell Signaling Technology, Inc.), ING2 (1:1,000; cat. no. 11560-1-AP; Proteintech Group, Inc.), p53 (1:5,000; cat. no. 10442-1-AP; Proteintech Group, Inc.) and β-actin (1:20,000; cat. no. 66009-1-Ig; Proteintech Group, Inc.) overnight at 4˚C. After washing, the membranes were incubated with the HRP goat anti-rabbit IgG (1:5,000; cat no. SA00001-2; Proteintech Group Inc.) or HRP-conjugated goat anti-mouse IgG (1:5,000; cat no. SA00001-1; Proteintech Group Inc.) at room temperature for 1 h. An ECL substrate (cat. no. E411-04; Vazyme Biotech Co., Ltd.) was used to visualize the protein bands and the data were analyzed using ImageJ 1.54g.

IHC. GC and adjacent noncancerous tissues previously preserved in 4% formalin were embedded, then the sections were prepared to a thickness of 5 μm. Subsequently, sections were permeabilized with 0.1% Triton X-100 (cat. no. T8200; Beijing Solarbio Science & Technology Co., Ltd.) at room temperature for 30 min, allowing antibodies to enter the cells, and endogenous peroxidase was blocked with 3% hydrogen peroxide at room temperature for 10 min. BSA (5%; cat. no. SW3015; Beijing Solarbio Science & Technology Co., Ltd.) was used to block non-specific binding sites at room temperature for 1 h. SMURF1 antibody (1:200; cat no. ab57573; Abcam) was used for IHC staining, and sections were incubated with this antibody overnight at 4˚C. The horseradish peroxidase-conjugated goat anti-mouse IgG (1:5,000; cat. no. ZB2305; Beijing Zhongshan Jinqiao Biotechnology Co., Ltd.) was used to incubate the sections at room temperature for 1 h. Chromogenic detection was performed using DAB (cat no. DA1010; Beijing Solarbio Science & Technology Co., Ltd.). Three fields were randomly selected to determine the percentage of positive cells and the staining intensity by light microscope. The expression grade of SMURF1 was calculated by multiplying the positivity score by the intensity score (21). Cells with <10% staining were rated as 1, cells with 10-49% staining were rated as 2, cells with 50-74% staining were rated as 3 and cells with 75-100% staining were rated as 4. The staining color was scored as light-yellow particles, 1; brown-yellow particles, 2; and brown particles, 3. The final score was defined as staining number score multiplied by staining color score. Patients were subsequently divided into high expression level (grade >3) and low expression level (grade ≤3) groups.

Dual-luciferase reporter assay. The miR-424-5p binding site in the 3'-UTR of SMURF1 was predicted using starBase v2.0 (http://starbase.sysu.edu.cn/). psiCHECK2-wild type (WT)-SMURF1 and psiCHECK2-mutant-SMURF1 were synthesized by Hanbio Biotechnology Co., Ltd. and were cotransfected with miR-424-5p mimics or nc into 293T cells (cat. no. CL-0005; Procell Life Science & Technology Co., Ltd) Lipofectamine 2000. After culture for 48 h, the dual-luciferase system (cat no. E2920; Promega Corporation) was used to measure the firefly luciferase (F-Luc) and *Renilla* luciferase (R-Luc) values, and the relative fluorescence values of firefly luciferase were calculated as F-Luc/R-Luc.

CCK-8 assay. The cells were inoculated into 96-well plates (4,000 cells/well) (Corning, Inc.) for 24 h. Then, the cells were treated with different concentrations (0, 0.005, 0.05, 0.5, 5, 50 and 500 μg/ml) of CDDP (cat. no. P4394; MilliporeSigma) for 48 h at 37˚C in a humidified atmosphere containing 5% CO_2. The CCK-8 assay (cat. no. CA1210; Beijing Solarbio Science & Technology Co., Ltd.) was used to measure cell viability and the half maximal inhibitory concentration (IC_{50}) was determined using GraphPad Prism 8 software (Dotmatics).

Flow cytometry. The cells were divided into an experimental group and a control group, and were seeded into 6-well plates ($1x10^5$ cells/well; Corning Life Sciences) for 24 h. The

experimental group was treated with CDDP (10 μg/ml in AGS cells and 2 μg/ml in HGC27 cells) for 48 h at 37˚C and the control group was treated with DMSO for the same duration. Annexin V-FITC/7-AAD (cat no. 40311ES60; Shanghai Yeasen Biotechnology Co., Ltd.) was used for apoptosis analysis; the samples were stained with Annexin V-FITC at room temperature for 5 min in the dark, after which, 7-AAD was added and the cells were immediately analyzed by flow cytometry (BD FACSCanto II; BD Biosciences). The data were analyzed using FlowJo (v10.8.1; FlowJo LLC) and GraphPad Prism 8 software. The apoptosis rate was represented by the sum of the early apoptotic rate and the late apoptotic rate.

Statistical analysis. SPSS version 26 (IBM Corp.) and GraphPad Prism 8 were used to analyze the data. The numerical data are presented as the mean ± standard deviation of at least three experimental repeats. The normality of the data was tested using the Kolmogorov-Smirnov test, and the comparisons among groups were analyzed using either unpaired or paired Student's t-test or one-way ANOVA followed by Bonferroni's post hoc test. Clinicopathological data were analyzed using the χ^2 test or Fisher's exact test. Correlations between variables were tested using linear regression and Spearman rank tests. $P<0.05$ was considered to indicate a statistically significant difference.

Results

miR-424-5p is downregulated in human GC tissues and cell lines. The expression of miR-424-5p in noncancerous gastric epithelial cells (GES-1) and GC cell lines (HGC27, MKN45, NCI-N87 and AGS) was assessed using RT-qPCR. As shown in Fig. 1A, the expression of miR-424-5p in GC cells was lower than that in GES-1 cells. In addition, 80 pairs of GC tissues and adjacent noncancerous tissues were collected and the absolute expression of miR-424-5p was assessed by miRNA RT-qPCR. Compared with those in paired adjacent tissues, the expression levels of miR-424-5p in human GC tissues were decreased (Fig. 1B). The samples were subsequently divided into high- and low-expression groups on the basis of their miR-424-5p expression levels, according to the median value. As shown in Table I, owing to one missing data point, 40 patients were included in the high-miR-424-5p group and 39 patients were included in the low-miR-424-5p group. Low miR-424-5p expression was associated with increased pathological N stage. The survival analysis of all samples revealed a weak association with poor prognostic outcome, but the results were not significant (Fig. 1C). Subgroup analysis revealed that lower expression of miR-424-5p was associated with a poor OS and RFS in patients treated with adjuvant chemotherapy (Fig. 1D).

miR-424-5p inhibits chemoresistance in GC cells. To investigate the effect of miR-424-5p on chemotherapy resistance in GC, the present study used AGS and HGC27 cells to verify the biological function of miR-424-5p. The results of miR-424-5p expression and the IC_{50} values of CDDP in AGS and HCG27 cells are shown in Fig. 2A. The IC_{50} value in AGS cells was greater than that in HGC27 cells, which indicated that AGS cells may be more resistant to CDDP than HGC27 cells. According to the miR-424-5p expression status in GC cells shown in Fig. 1A, miR-424-5p exhibited the highest expression in HGC27 cells, whereas its expression was the lowest in AGS cells. Therefore, the HGC27 cells were selected for miR-424-5p silencing, while AGS cells were chosen for miR-424-5p overexpression in subsequent experiments. The miR-424-5p mimics and inhibitor were constructed and transfected into AGS and HGC27 cells, respectively. RT-qPCR was performed to verify the transfection efficiency in the cell lines (Fig. 2B). As expected, miR-424-5p was significantly upregulated in AGS cells and significantly downregulated in HGC27 cells post-transfection compared with that in the nc groups. First, the colony formation, wound healing, Transwell and invasion assays revealed that there was no significant difference in cell proliferation, invasion and migration after altering the expression of miR-424-5p (Fig. S2). A CCK-8 assay, flow cytometry and western blotting were used to evaluate the effects of miR-424-5p on CDDP resistance in GC cells. The CCK-8 assay results revealed that the sensitivity of AGS cells transfected with the miR-424-5p mimics to CDDP was increased compared with that of the cells transfected with miR-nc, whereas HGC27 cells transfected with the miR-424-5p inhibitor presented the opposite results (Fig. 2C and D). Following CDDP treatment, flow cytometry revealed that the apoptosis rate of the miR-424-5p mimics-transfected cells was greater than that of the miR-nc-transfected cells (Fig. 2E). By contrast, a lower percentage of apoptotic cells was detected in the miR-424-5p inhibitor group (Fig. 2F). In addition, to evaluate apoptosis, the expression levels of caspase 3 and cleaved caspase 3 were assessed. In contrast to the nc groups, the cleaved caspase 3/caspase 3 rate was elevated in the miR-424-5p mimics group and was reduced in the miR-424-5p inhibitor group, which indicated that the miR-424-5p could promote apoptosis following CDDP treatment (Fig. 2G and H).

SMURF1 is a target gene of miR-424-5p. In our previous study, SMURF1 was found to be downstream of miR-424-5p (11). The miR-424-5p binding site in the 3'-UTR of SMURF1 was predicted using starBase v2.0. A dual-luciferase reporter assay revealed that the luciferase activity in the SMURF1 3'UTR WT group was significantly lower than that in the nc group ($P<0.05$; Fig. 3A). Thus, these results confirmed that miR-424-5p regulated luciferase expression through this binding site. To clarify the mechanism by which miR-424-5p regulates SMURF1 in GC, RT-qPCR and western blotting were used to assess the expression levels of SMURF1 in different treatment groups. The qPCR results revealed that the mRNA expression levels of SMURF1 in AGS cells transfected with miR-424-5p mimics were significantly lower than those in the miR-nc group (Fig. 3B). By contrast, the mRNA expression levels of SMURF1 in HGC27 cells transfected with the miR-424-5p inhibitor were significantly increased. Consistently, the western blotting results were the same as the RT-qPCR results. These results suggested that miR-424-5p may suppress the expression of SMURF1.

SMURF1 is upregulated in human GC tissues and cell lines. The present study next assessed the expression of SMURF1

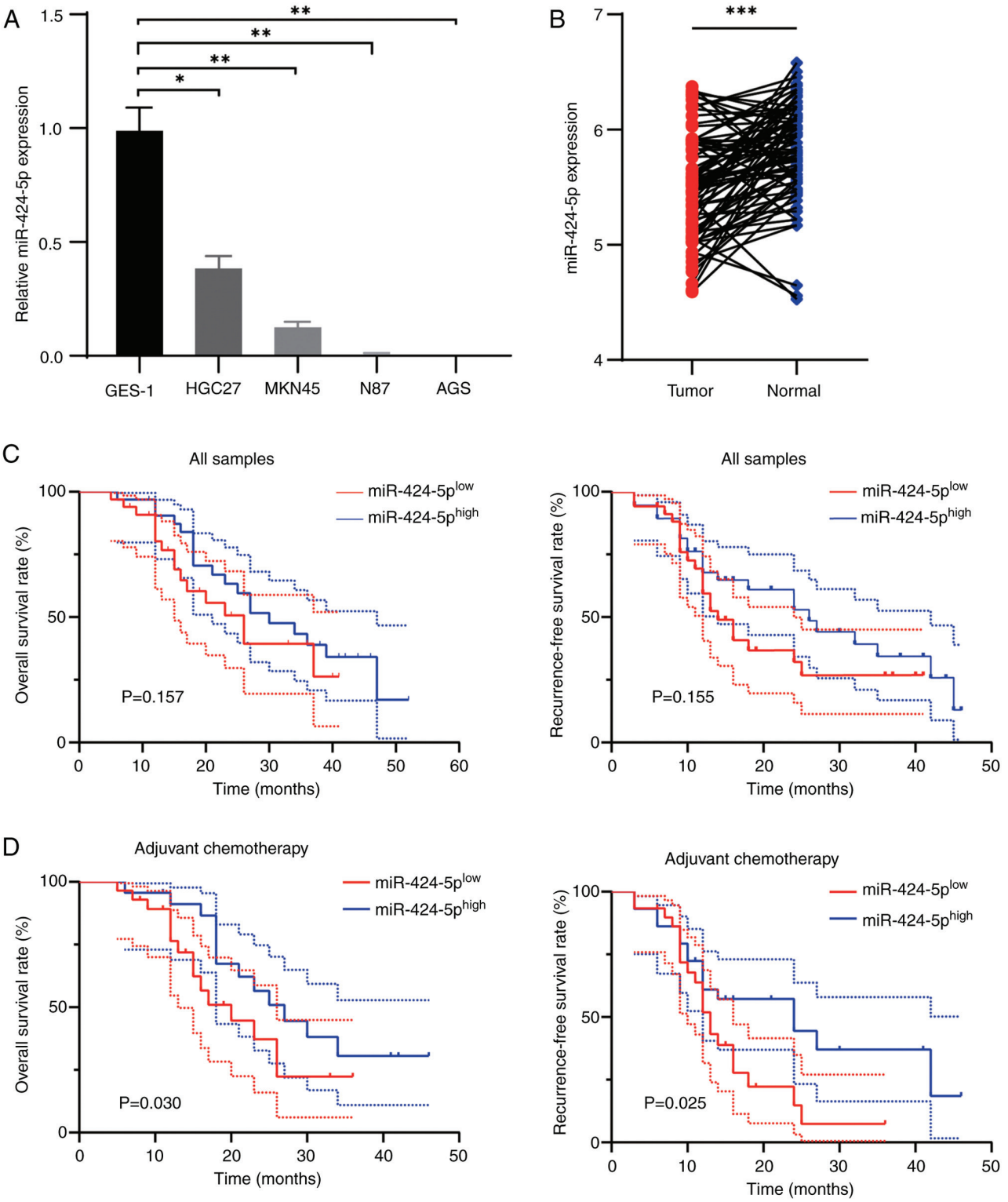

Figure 1. Expression of miR-424-5p and survival analysis. (A) Relative expression levels of miR-424-5p in GC cells and GES-1 cells were determined by RT-qPCR. (B) Expression levels of miR-424-5p in 80 pairs of GC tissues and adjacent noncancerous tissues determined by RT-qPCR. (C) Survival analysis was performed for all patients. (D) Subgroup analysis of overall survival and recurrence-free survival. *P<0.05, **P<0.01, ***P<0.001. miR, microRNA; GC, gastric cancer; RT-qPCR, reverse transcription-quantitative PCR.

in GC cell lines and GES-1 cells by RT-qPCR and western blotting. As shown in Fig. 4A and B, the mRNA expression levels of SMURF1 in GC cells, such as NCI-N87, AGS and MKN45, were greater than those in GES-1 cells, while SMURF1 protein levels were higher in NCI-N87, AGS, MKN45 and HGC27 cells. IHC analysis revealed that SMURF1 was expressed at higher levels in GC tissues than in adjacent tissues (Fig. 4C). Furthermore, miR-424-5p was revealed to be negatively correlated with SMURF1 in GC tissues, although the correlation was weak (Fig. 4D). In addition, the association between SMURF1 expression levels and clinicopathological characteristics was analyzed.

Table I. Association between expression levels of miR-424-5p and SMURF1 and the clinicopathological characteristics of patients.

	miR-424-5p expression			SMURF1 expression		
Characteristic	Low	High group	P-value	Low	High group	P-value
Male sex, n (%)	26 (68.4)	31 (75.6)	0.476[b]	32 (66.7)	25 (80.6)	0.176[b]
Aged ≥60 years, n (%)	33 (86.8)	31 (75.6)	0.203[b]	41 (85.4)	23 (74.2)	0.214[b]
Location			0.635[b]			0.058[b]
Upper	5 (13.2)	8 (19.5)		7 (14.6)	6 (19.4)	
Body	9 (23.7)	7 (17.1)		6 (12.5)	10 (32.3)	
Lower	24 (63.2)	26 (63.4)		35 (72.9)	15 (48.4)	
Sized >3 cm, n (%)	20 (52.6)	20 (48.8)	0.732[b]	21 (43.8)	19 (61.3)	0.128[b]
T grade			0.767[a]			0.312[a]
I	3 (7.9)	6 (14.6)		7 (14.6)	2 (6.5)	
II	5 (13.2)	6 (14.6)		8 (16.7)	3 (9.7)	
III	6 (15.8)	7 (17.1)		9 (18.8)	4 (12.9)	
IV	24 (63.2)	22 (53.7)		24 (50.0)	22 (71.0)	
N grade			0.009[b]			0.336[b]
0	6 (15.8)	18 (43.9)		18 (37.5)	6 (19.4)	
1	5 (13.2)	9 (22.0)		8 (16.7)	6 (19.4)	
2	9 (23.7)	6 (14.6)		9 (18.8)	6 (19.4)	
3	18 (47.4)	8 (19.5)		13 (27.1)	13 (41.9)	
M grade			0.140[a]			0.075[a]
0	34 (89.5)	40 (97.6)		47 (97.9)	27 (87.1)	
1	4 (10.5)	1 (2.4)		1 (2.1)	4 (12.9)	
TNM stage			0.058[a]			0.020[a]
I	4 (10.5)	9 (22.0)		10 (20.8)	3 (9.7)	
II	5 (13.2)	12 (29.3)		14 (29.2)	3 (9.7)	
III	25 (65.8)	19 (46.3)		23 (47.9)	21 (67.7)	
IV	4 (10.5)	1 (2.4)		1 (2.1)	4 (12.9)	
Histological type			0.115[a]			0.141[a]
Poorly	21 (55.3)	30 (73.2)		27 (56.3)	24 (77.4)	
Moderately	12 (31.6)	10 (24.4)		17 (35.4)	5 (16.1)	
Well	5 (13.2)	1 (2.4)		4 (8.3)	2 (6.5)	

[a]Calculated by Fisher's exact test and [b]χ^2 test. miR, microRNA; SMURF1, SMAD-specific E3 ubiquitin protein ligase 1; TNM, Tumor-Node-Metastasis.

High expression of SMURF1 was associated with increased Tumor-Node-Metastasis stage (Table I).

miR-424-5p suppresses SMURF1 protein expression via mRNA degradation. The present study confirmed that miR-424-5p regulated CDDP resistance in GC cells. To further confirm whether miR-424-5p regulated drug resistance in GC cells by partially inhibiting SMURF1 expression, AGS cells overexpressing SMURF1 and HGC27 cells with SMURF1 knockdown were constructed, and the effects of its overexpression and knockdown were verified by RT-qPCR and western blotting (Fig. S3). In addition, the expression of miR-424-5p was detected by RT-qPCR following SMURF1 knockdown or overexpression and it was found that the knockdown or overexpression of SMURF1 did not influence miR-424-5p expression (Fig. S4). Then, four groups of AGS cells, namely, the miR-nc + LV-nc, miR-424-5p mimics + LV-nc, miR-nc + LV-SMURF1 and miR-424-5p mimics + LV-SMURF1 groups, were constructed via cotransfection. Similarly, miR-nc + sh-nc, miR-424-5p inhibitor + sh-nc, miR-nc + sh-SMURF1 and miR-424-5p inhibitor + sh-SMURF1 HGC27 cells were constructed. In terms of drug response, the CCK-8 assay results revealed that CDDP resistance was increased after SMURF1 was upregulated in AGS cells and decreased after SMURF1 was downregulated in HGC27 cells (Fig. 5A and B). The CDDP resistance induced by LV-SMURF1 could be reversed by overexpressing miR-424-5p in GC cells. By contrast, the CDDP sensitivity induced by sh-SMURF1 was not be altered by the miR-424-5p inhibitor. In addition, flow cytometry demonstrated that the overexpression of SMURF1 in GC cells reduced the number of apoptotic GC cells and this effect was

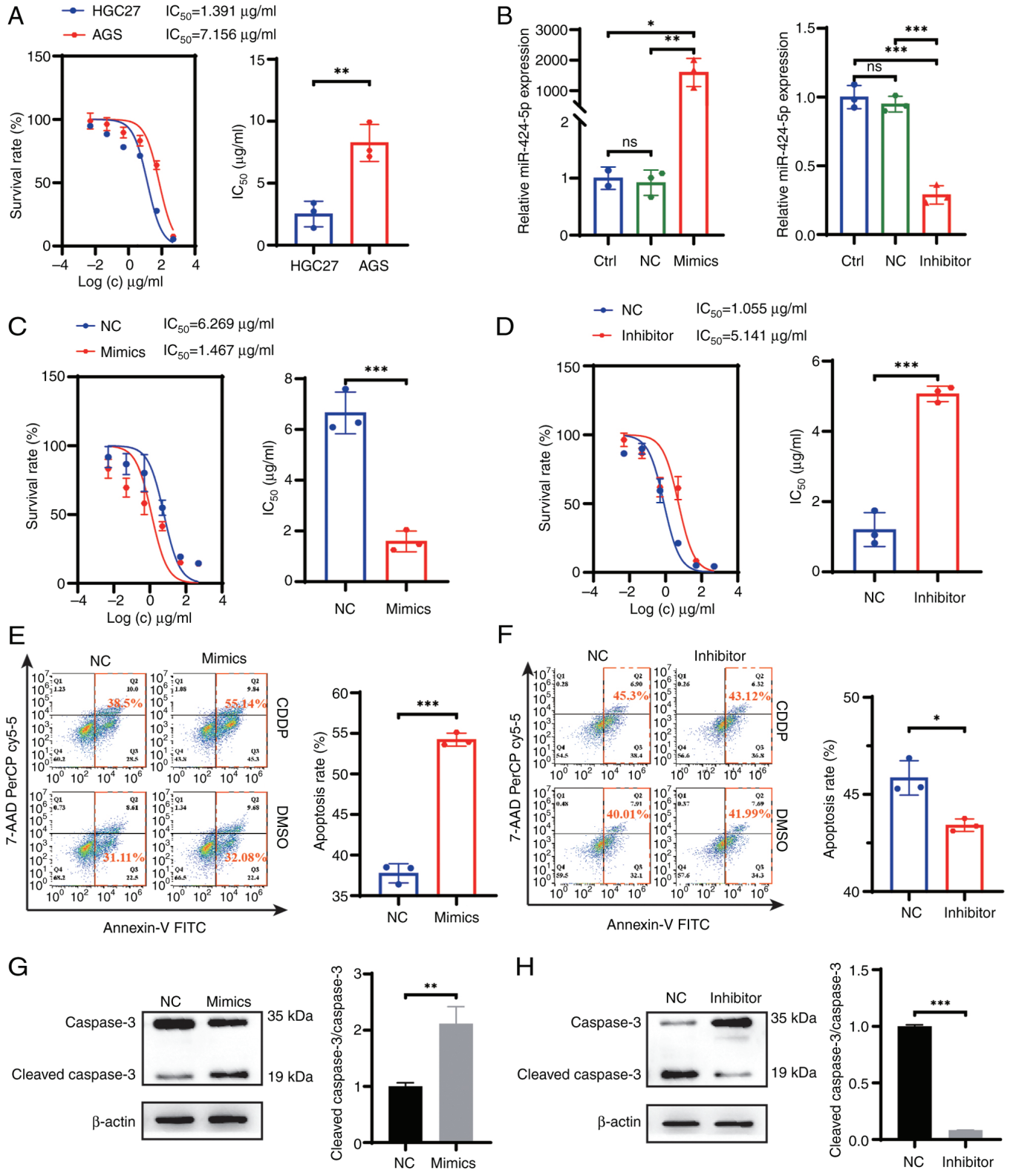

Figure 2. Relationship between the expression levels of miR-424-5p and CDDP resistance. (A) IC_{50} values of CDDP in HGC27 and AGS cells were determined using the Cell Counting Kit-8 assay. (B) Expression of miR-424-5p in AGS and HGC7 cells following transfection with the miR-424 mimics, the miR-424 inhibitor or the corresponding ncs. IC_{50} values of CDDP in (C) AGS and (D) HGC27 cells following overexpression or inhibition of miR-424-5p. The percentages of Annexin V-positive cells upon treatment with (E) 10 μg/ml CDDP in AGS cells and (F) 1.5 μg/ml CDDP in HGC27 cells; after 48 h, the cells were examined by flow cytometry. Caspase 3 and cleaved caspase 3 expression levels were detected by western blotting following treatment with CDDP or DMSO in (G) AGS and (H) HGC27 cells. *P<0.05, **P<0.01, ***P<0.001. miR, microRNA; CDDP, cisplatin; IC_{50}, half maximal inhibitory concentration; nc, negative control; ns, not significant.

reversed by the transfection of miR-424-5p mimics (Fig. 5C). Moreover, the miR-424-5p inhibitor was found to reduce the apoptosis rate. By contrast, sh-SMURF1 increased the apoptosis rate, and this could be slightly attenuated by the

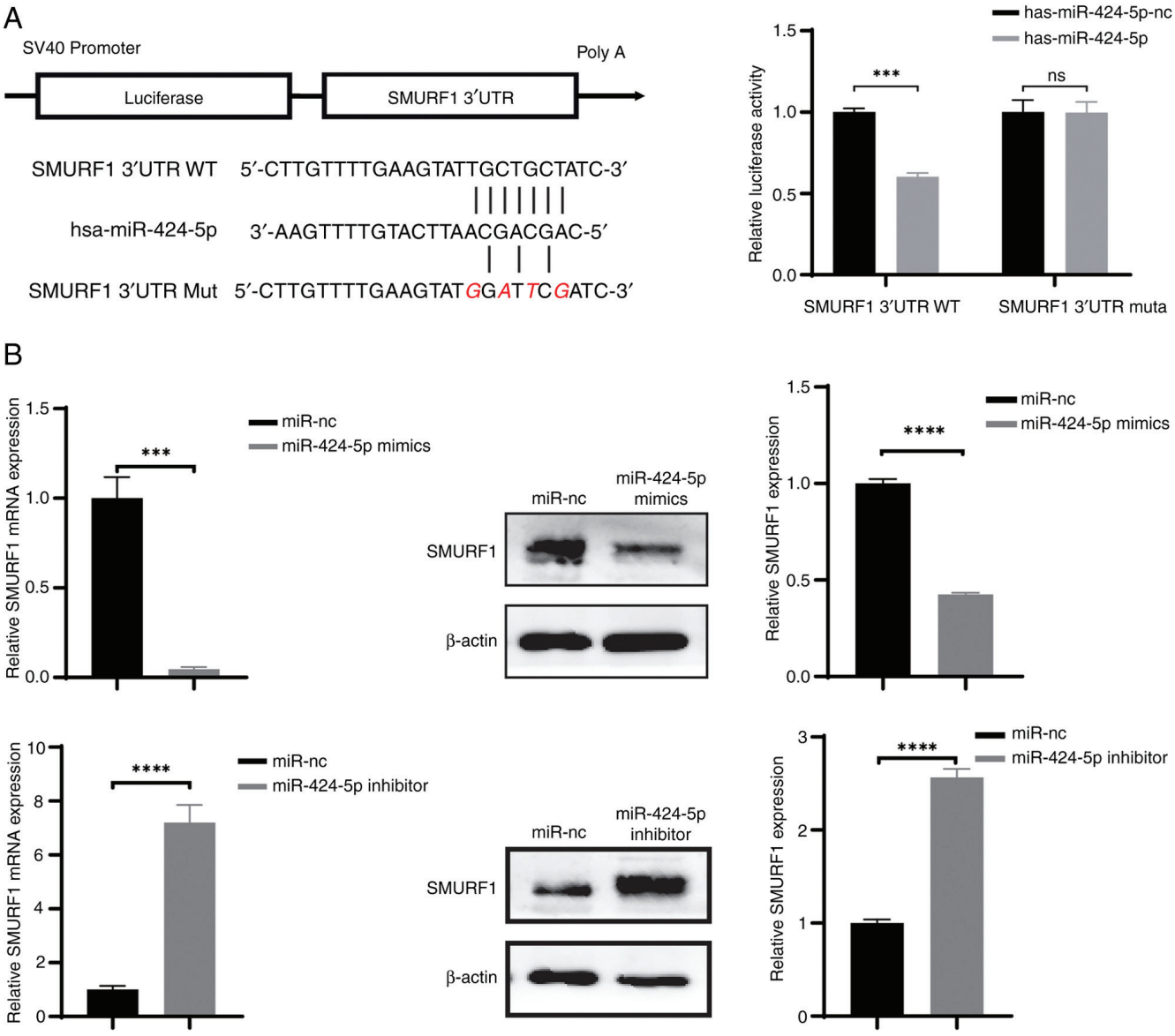

Figure 3. Luciferase reporter assay and expression of SMURF1 in transfected cells. (A) SMURF1 was confirmed to be a direct target gene of miR-424-5p. (B) Reverse transcription-quantitative PCR and western blot analysis of SMURF1 after cell transfection. ***P<0.001, ****P<0.0001. SMURF1, SMAD-specific E3 ubiquitin protein ligase 1; miR, microRNA; WT, wild type; muta, mutant; nc, negative control; ns, not significant.

miR-424-5p inhibitor (Fig. 5D). The western blotting results revealed a consistent trend in caspase 3 changes; the effects of SMURF1 expression on apoptosis in response to CDDP treatment were validated by the protein expression levels of cleaved caspase 3. The results indicated that miR-424-5p mimics enhanced the cleaved caspase 3/caspase 3 ratio. By contrast, SMURF1 overexpression significantly reduced this ratio, an effect that could be reversed by miR-424-5p mimics. Similarly, the miR-424-5p inhibitor decreased the cleaved caspase 3/caspase 3 ratio, whereas sh-SMURF1 increased the ratio, with this increase being modestly attenuated by the miR-424-5p inhibitor (Fig. 6A and B).

p53 serves an important role in chemosensitivity and ING2 activates p53 in neoplasms. Moreover, SMURF1 interacts with and targets ING2 for polyubiquitination and proteasomal degradation (14). Western blotting data revealed that the protein expression levels of ING2 and p53 were partially inhibited or promoted by the miR-424-5p mimics or inhibitor, respectively (Fig. 6C and D). It was found that the expression of ING2 and p53 in AGS cells transfected with LV-SMURF1 decreased and this change nearly disappeared following transfection with the miR-424-5p mimics. Similarly, the levels of ING2 and p53 were increased in HGC27 cells transfected with sh-SMURF1 and were partially restored by transfection with the miR-424-5p inhibitor. These results indicated that the overexpression of miR-424-5p may inhibit the expression levels of SMURF1 and increase the expression levels of p53.

Discussion

CDDP-based chemotherapy is currently the standard of care for patients with GC; however, consequent chemotherapy insensitivity and resistance may lead to tumor progression, treatment failure and poor prognosis (22,23). The development

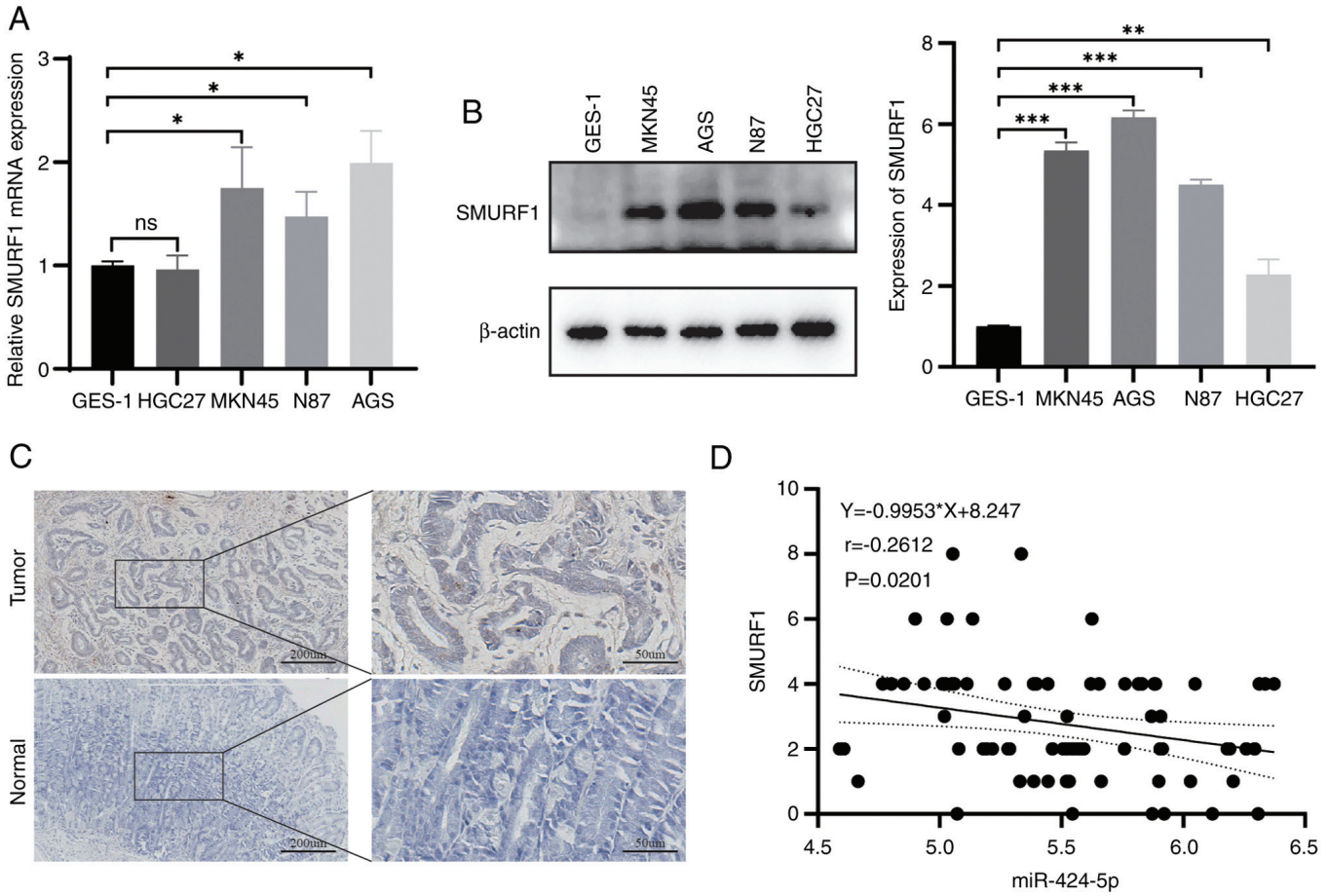

Figure 4. SMURF1 expression in GC cells and GC tissues. (A) Relative expression levels of SMURF1 in GC cells and GES-1 cells were determined by reverse transcription-quantitative PCR. (B) Relative expression levels of SMURF1 in GC cells and GES-1 cells were determined by western blotting. (C) Expression of SMURF1 in GC tissues compared with adjacent tissues. (D) Correlation between the expression of SMURF11 and the expression of miR-424-5p. *P<0.05, **P<0.01, ***P<0.001. SMURF1, SMAD-specific E3 ubiquitin protein ligase 1; GC, gastric cancer; miR, microRNA; ns, not significant.

of treatment resistance is related to the expression of multi-drug resistance genes, and abnormalities in apoptosis, the cell cycle and autophagy in tumor cells (24-26). A large amount of evidence has suggested that miRNAs are involved in the development of cancer and that they also serve important roles in the resistance of GC to chemotherapy drugs and targeted therapy drugs (27,28). Various oncogenic miRNAs, such as miR-20a, miR-193a and miR-30, have been reported to promote the resistance of GC cells to CDDP (27,29,30). The present study found that miR-424-5p was expressed at low levels in GC cells and inhibited CDDP resistance in GC cells through a series of experiments. In addition, it was revealed via clinicopathological data that low miR-424-5p expression was related to the degree of malignancy of the tumor. These findings provided new targets for the treatment of chemotherapy resistance in GC.

miRNAs are important noncoding RNAs that regulate the expression of various genes (4,31). Notably, miRNAs regulate apoptosis in colorectal tumors (32) and miR-424-5p has been shown to serve roles in different diseases (33,34). miR-424-5p is particularly relevant to tumor prognosis and has an important role in early diagnosis and treatment. Studies have shown that miR-424-5p can be used as a biomarker to predict the prognosis of patients with pancreatic cancer, liver cancer or non-small cell lung cancer (35-37). Accumulating evidence has also shown that miR-424-5p is involved in regulating cellular functions, such as cell proliferation, migration and invasion. For example, miR-424-5p has been shown to inhibit epithelial-mesenchymal transition in glioma by targeting KIF23 (38). In cervical cancer, miR-424-5p can target KDM5B through the NOTCH1 signaling pathway to affect proliferation, and regulate CHK1 to alter migration, invasion, apoptosis and the cell cycle (39,40). In addition, miR-424 can increase the sensitivity of ovarian cancer cells to CDDP by inhibiting the expression of galectin-3 (41), while Geretto *et al* (42) reported that miR-424 may increase the sensitivity of tumors to docetaxel. Moreover, miR-424 has been demonstrated to block the PD-L1 immune checkpoint and reactivate the T-cell immune response, enhancing immune-killing effects and attenuating drug resistance (43). Our previous analysis of the GEO database revealed that miR-424-5p may regulate CDDP resistance in GC by targeting SMURF1 expression (11). Therefore, the present study confirmed this hypothesis using *in vitro* experiments. It first studied the effects of miR-424-5p on cell proliferation, migration and invasion, but the results were not statistically significant. The present study demonstrated that the expression levels of miR-424-5p in GC cells were negatively associated with the IC_{50} of CDDP and that its sensitivity to CDDP was affected by the overexpression or inhibition of intracellular miR-424-5p expression, which could be restored by the overexpression or knockdown of SMURF1.

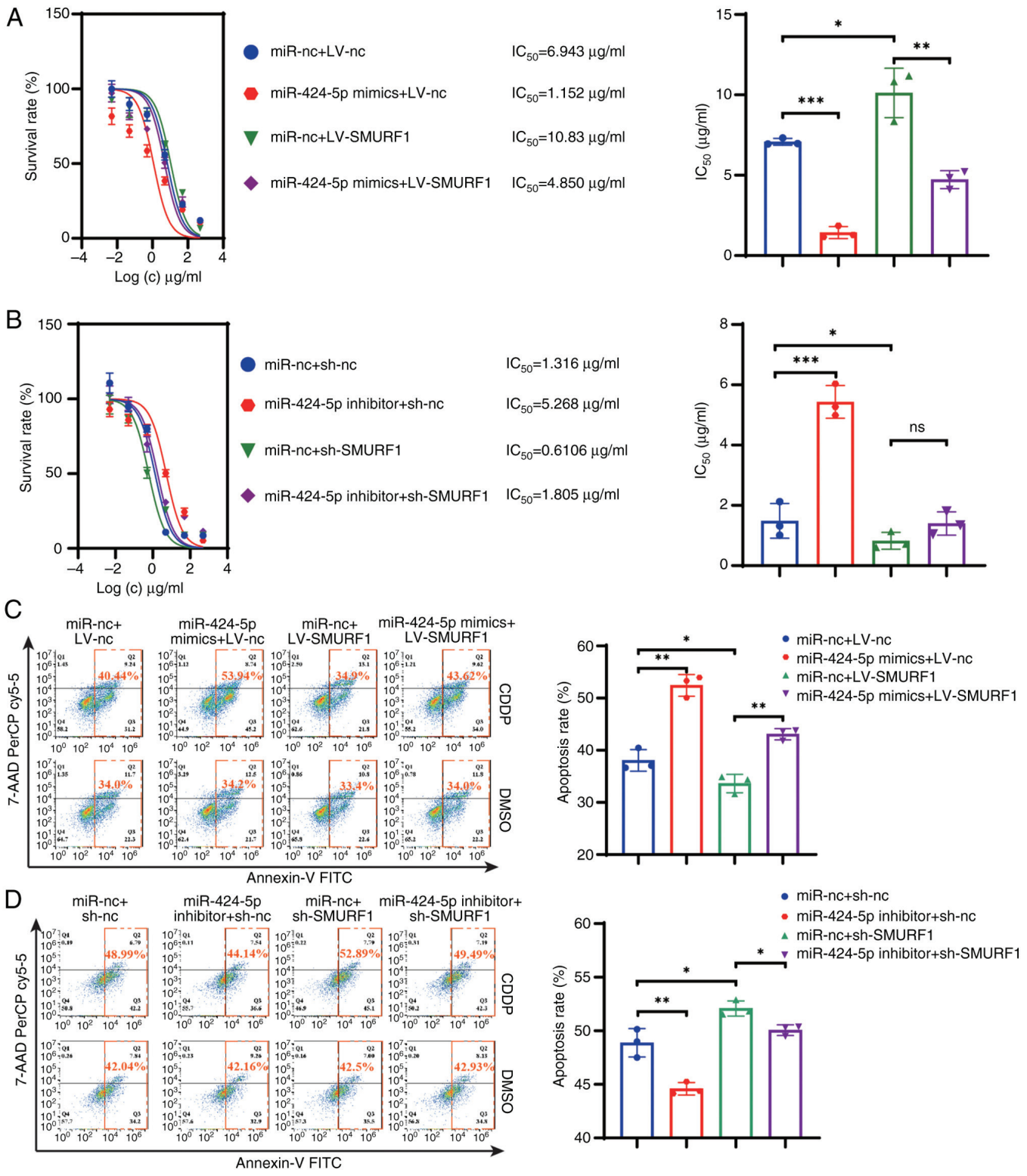

Figure 5. miR-424-5p regulates CDDP resistance. IC_{50} values of CDDP in the (A) AGS and (B) HGC27 groups. The percentages of Annexin V-positive cells in the (C) AGS and (D) HGC27 groups were detected by flow cytometry. $^{*}P<0.05$, $^{**}P<0.01$, $^{***}P<0.001$. miR, microRNA; CDDP, cisplatin; IC_{50}, half maximal inhibitory concentration; nc, negative control; sh, short hairpin; LV, lentivirus; ns, not significant.

In addition, the present study explored the specific mechanism by which miR-424-5p affects CDDP resistance in GC cells after SMURF1 is modulated. SMURF1, a ubiquitin ligase, was first shown to regulate the Smad protein in the TGFβ/BMP signaling pathway (44). Recently, in-depth research on ubiquitination-mediated cancer progression and development has been performed. The function of SMURF1 as a potential protooncogene has also been identified. SMURF1 promotes tumor metastasis and inhibits apoptosis in GC, prostate cancer and ovarian cancer (15,45). In addition, in patient-derived xenograft models, SMURF1 has been revealed to be associated with sensitivity to CDDP

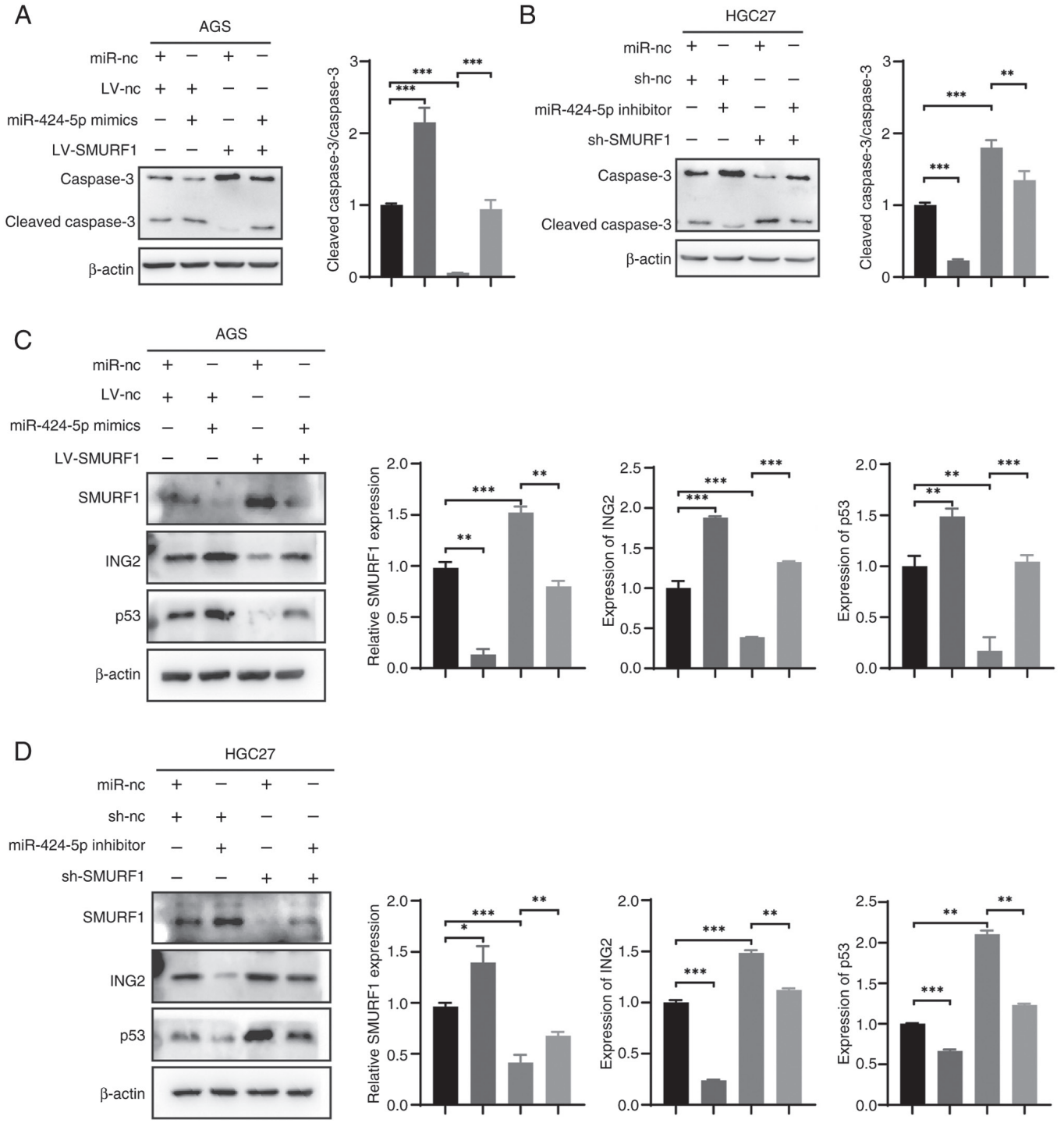

Figure 6. miR-424-5p regulates CDDP resistance through the SMURF1/ING2/P53 axis. Western blotting of caspase 3 and cleaved caspase 3 in the (A) AGS and (B) HGC27 cells. Changes in SMURF1/ING2/P53 detected by western blotting in the (C) AGS and (D) HGC27 cells. *P<0.05, **P<0.01, ***P<0.001. miR, microRNA; CDDP, cisplatin; SMURF1, SMAD-specific E3 ubiquitin protein ligase 1; nc, negative control; LV, lentivirus.

chemotherapy in colorectal cancer (46). The present study provided further evidence that the inhibition of SMURF1 may improve the efficacy of chemotherapy in GC cells. In response to the inhibition of SMURF1 by the overexpression of miR-424-5p, the IC_{50} of CDDP in GC cells decreased, whereas CDDP-induced apoptosis increased. A previous study has shown that SMURF1 regulates apoptosis by interacting with ING2 through the HECT domain (14). ING2 interacts with p53, enhances the transcriptional activity of p53 and regulates cellular senescence, apoptosis and the DNA damage response (47). The present study found that miR-424-5p inhibited SMURF1 expression, which in turn affected the expression of ING2 and p53, ultimately regulating CDDP resistance in GC cells.

In summary, the present study demonstrated that SMURF1 is a target of miR-424-5p, and contributes to regulating cell survival and death by regulating apoptosis. In GC, miR-424-5p inhibited SMURF1 expression by

binding to the 3'-UTR of SMURF1, which may increase p53 expression. p53 is an important regulator of apoptosis in the CDDP-mediated damage response. Therefore, miR-424-5p may increase the levels of p53 and thus increase apoptosis and the sensitivity of GC cells to CDDP treatment. However, a limitation of the present study was the absence of mechanistic experiments in animal models to validate the regulatory effects of the miR-424-5p/SMURF1/ING2/p53 axis on CDDP resistance. In the future, the effects of miR-424-5p on the tumor immune microenvironment will be explored. Subsequently, nanocarriers will be developed for the targeted delivery of miR-424-5p to overcome drug resistance in GC.

In conclusion, the present study revealed that miR-424-5p regulates chemoresistance via the miR-424-5p/SMURF1/ING2/p53 axis in GC. Thus, the development of drugs that target miR-424-5p during tumor therapy may ultimately improve the response of patients with GC to chemotherapeutic agents.

Acknowledgements

Not applicable.

Funding

The present study was supported by the National Natural Science Foundation of China (approval no. 82003301) and the Tianjin Municipal Education Commission's research project (approval no. 2023KJ117).

Availability of data and materials

The data generated in the present study may be requested from the corresponding author.

Authors' contributions

Conceptualization was performed by LL and WF, the methodology was designed by DW, data analysis was performed by HC, and formal analysis and investigation by DW. YY participated in the acquisition and analysis of data. DW was responsible for writing, reviewing and editing the manuscript and LL was responsible for visualization. LL and WF confirm the authenticity of all the raw data. All authors read and approved the final version of the manuscript.

Ethics approval and consent to participate

The present study was conducted in accordance with The Declaration of Helsinki and approved by the Ethics Committee of Tianjin Medical University General Hospital (approval no. IRB2020-KY-640). Written informed consent was obtained from all patients or their relatives for specimen collection.

Patient consent for publication

Written informed consent was obtained from the patients for their anonymized information to be published in this article.

Competing interests

The authors declare that they have no competing interests.

References

1. Sung H, Ferlay J, Siegel RL, Laversanne M, Soerjomataram I, Jemal A and Bray F: Global cancer statistics 2020: GLOBOCAN estimates of incidence and mortality worldwide for 36 cancers in 185 countries. CA Cancer J Clin 71: 209-249, 2021.
2. Smyth EC, Nilsson M, Grabsch HI, van Grieken NC and Lordick F: Gastric cancer. Lancet 396: 635-648, 2020.
3. Wei L, Sun J, Zhang N, Zheng Y, Wang X, Lv L, Liu J, Xu Y, Shen Y and Yang M: Noncoding RNAs in gastric cancer: Implications for drug resistance. Mol Cancer 19: 62, 2020.
4. Rupaimoole R and Slack FJ: MicroRNA therapeutics: Towards a new era for the management of cancer and other diseases. Nat Rev Drug Discov 16: 203-222, 2017.
5. Zhang Q, Zhuang J, Deng Y, Yang L, Cao W, Chen W, Lin T, Lv X, Yu H, Xue Y and Guo H: miR34a/GOLPH3 axis abrogates urothelial bladder cancer chemoresistance via reduced cancer stemness. Theranostics 7: 4777-4790, 2017.
6. Peng Y, Hu S, Zhang K, Wang Y, Rouzi M, Zhou D and Yang R: Downregulation of microRNA-130a inhibits oral squamous cell carcinoma proliferation and metastasis via the hippo-YAP pathway. Cancer Manag Res 13: 4829-4840, 2021.
7. Wiggins JF, Ruffino L, Kelnar K, Omotola M, Patrawala L, Brown D and Bader AG: Development of a lung cancer therapeutic based on the tumor suppressor microRNA-34. Cancer Res 70: 5923-5930, 2010.
8. Liu C, Kelnar K, Liu B, Chen X, Calhoun-Davis T, Li H, Patrawala L, Yan H, Jeter C, Honorio S, *et al*: The microRNA miR-34a inhibits prostate cancer stem cells and metastasis by directly repressing CD44. Nat Med 17: 211-215, 2011.
9. Trang P, Wiggins JF, Daige CL, Cho C, Omotola M, Brown D, Weidhaas JB, Bader AG and Slack FJ: Systemic delivery of tumor suppressor microRNA mimics using a neutral lipid emulsion inhibits lung tumors in mice. Mol Ther 19: 1116-1122, 2011.
10. Feng J, Lu SS, Xiao T, Huang W, Yi H, Zhu W, Fan S, Feng XP, Li JY, Yu ZZ, *et al*: ANXA1 binds and stabilizes EphA2 to promote nasopharyngeal carcinoma growth and metastasis. Cancer Res 80: 4386-4398, 2020.
11. Lu L, Wu M, Lu Y, Zhao Z, Liu T, Fu W and Li W: MicroRNA-424 regulates cisplatin resistance of gastric cancer by targeting SMURF1 based on GEO database and primary validation in human gastric cancer tissues. Onco Targets Ther 12: 7623-7636, 2019.
12. Narayanan S, Cai CY, Assaraf YG, Guo HQ, Cui Q, Wei L, Huang JJ, Ashby CR Jr and Chen ZS: Targeting the ubiquitin-proteasome pathway to overcome anti-cancer drug resistance. Drug Resist Updat 48: 100663, 2020.
13. Xia Q, Li Y, Han D and Dong L: SMURF1, a promoter of tumor cell progression? Cancer Gene Ther 28: 551-565, 2021.
14. Nie J, Liu L, Wu M, Xing G, He S, Yin Y, Tian C, He F and Zhang L: HECT ubiquitin ligase Smurf1 targets the tumor suppressor ING2 for ubiquitination and degradation. FEBS Lett 584: 3005-3012, 2010.
15. Fu L, Cui CP, Zhang X and Zhang L: The functions and regulation of Smurfs in cancers. Semin Cancer Biol 67: 102-116, 2020.
16. Xia Q, Zhang H, Zhang P, Li Y, Xu M, Li X, Li X and Dong L: Oncogenic Smurf1 promotes PTEN wild-type glioblastoma growth by mediating PTEN ubiquitylation. Oncogene 39: 5902-5915, 2020.
17. Khammanivong A, Gopalakrishnan R and Dickerson EB: SMURF1 silencing diminishes a CD44-high cancer stem cell-like population in head and neck squamous cell carcinoma. Mol Cancer 13: 260, 2014.
18. Rich JT, Neely JG, Paniello RC, Voelker CC, Nussenbaum B and Wang EW: A practical guide to understanding Kaplan-Meier curves. Otolaryngol Head Neck Surg 143: 331-336, 2010.
19. Heid CA, Stevens J, Livak KJ and Williams PM: Real time quantitative PCR. Genome Res 6: 986-894, 1996.
20. Livak KJ and Schmittgen TD: Analysis of relative gene expression data using real-time quantitative PCR and the 2-ΔΔCT method. Methods 25: 402-408, 2001.
21. Guo Z, Zhang X, Zhu H, Zhong N, Luo X, Zhang Y, Tu F, Zhong J, Wang X, He J and Huang L: TELO2 induced progression of colorectal cancer by binding with RICTOR through mTORC2. Oncol Rep 45: 523-534, 2021.

22. An Y, Wang B, Wang X, Dong G, Jia J and Yang Q: SIRT1 inhibits chemoresistance and cancer stemness of gastric cancer by initiating an AMPK/FOXO3 positive feedback loop. Cell Death Dis 11: 115, 2020.
23. Yang W, Ma J, Zhou W, Cao B, Zhou X, Yang Z, Zhang H, Zhao Q, Fan D and Hong L: Molecular mechanisms and theranostic potential of miRNAs in drug resistance of gastric cancer. Expert Opin Ther Targets 21: 1063-1075, 2017.
24. Czabotar PE, Lessene G, Strasser A and Adams JM: Control of apoptosis by the BCL-2 protein family: Implications for physiology and therapy. Nat Rev Mol Cell Biol 15: 49-63, 2014.
25. Hammond WA, Swaika A and Mody K: Pharmacologic resistance in colorectal cancer: A review. Ther Adv Med Oncol 8: 57-84, 2016.
26. Nies AT, Magdy T, Schwab M and Zanger UM: Role of ABC transporters in fluoropyrimidine-based chemotherapy response. Adv Cancer Res 125: 217-243, 2015.
27. Lee SD, Yu D, Lee DY, Shin HS, Jo JH and Lee YC: Upregulated microRNA-193a-3p is responsible for cisplatin resistance in CD44(+) gastric cancer cells. Cancer Sci 110: 662-673, 2019.
28. Zhu C, Huang Q and Zhu H: miR-383 inhibited the cell cycle progression of gastric cancer cells via targeting cyclin E2. DNA Cell Biol 38: 849-856, 2019.
29. Zhu M, Zhou X, Du Y, Huang Z, Zhu J, Xu J, Cheng G, Shu Y, Liu P, Zhu W and Wang T: miR-20a induces cisplatin resistance of a human gastric cancer cell line via targeting CYLD. Mol Med Rep 14: 1742-1750, 2016.
30. Du X, Liu B, Luan X, Cui Q and Li L: miR-30 decreases multidrug resistance in human gastric cancer cells by modulating cell autophagy. Exp Ther Med 15: 599-605, 2018.
31. Pillai RS, Bhattacharyya SN and Filipowicz W: Repression of protein synthesis by miRNAs: How many mechanisms? Trends Cell Biol 17: 118-126, 2007.
32. Wang H: MicroRNAs and apoptosis in colorectal cancer. Int J Mol Sci 21: 5353, 2020.
33. Min KH, Yang WM and Lee W: Saturated fatty acids-induced miR-424-5p aggravates insulin resistance via targeting insulin receptor in hepatocytes. Biochem Biophys Res Commun 503: 1587-1593, 2018.
34. Cheng D, Zhu C, Liang Y, Xing Y and Shi C: MiR-424 overexpression protects alveolar epithelial cells from LPS-induced apoptosis and inflammation by targeting FGF2 via the NF-kappaB pathway. Life Sci 242: 117213, 2020.
35. Wang Y, Lv Z, Fu J, Wang Z, Fan Z and Lei T: Endogenous microRNA-424 predicts clinical outcome and its inhibition acts as cancer suppressor in human non-small cell lung cancer. Biomed Pharmacother 89: 208-214, 2017.
36. Wu L, Yang F, Lin B, Chen X, Yin S, Zhang F, Xie H, Zhou L and Zheng S: MicroRNA-424 expression predicts tumor recurrence in patients with hepatocellular carcinoma following liver transplantation. Oncol Lett 15: 9126-9132, 2018.
37. Wang ZX, Deng TX and Ma Z: Identification of a 4-miRNA signature as a potential prognostic biomarker for pancreatic adenocarcinoma. J Cell Biochem 120: 16416-16426, 2019.
38. Zhao C, Wang XB, Zhang YH, Zhou YM, Yin Q and Yao WC: MicroRNA-424 inhibits cell migration, invasion and epithelial-mesenchymal transition in human glioma by targeting KIF23 and functions as a novel prognostic predictor. Eur Rev Med Pharmacol Sci 22: 6369-6378, 2018.
39. Xu J, Li Y, Wang F, Cheng B, Ye F, Xie X, Zhou C and Lu W: Suppressed miR-424 expression via upregulation of target gene Chk1 contributes to the progression of cervical cancer. Oncogene 32: 976-987, 2013.
40. Zhou Y, An Q, Guo RX, Qiao YH, Li LX, Zhang XY and Zhao XL: miR-424-5p functions as an anti-oncogene in cervical cancer cell growth by targeting KDM5B via the Notch signaling pathway. Life Sci 171: 9-15, 2017.
41. Bieg D, Sypniewski D, Nowak E and Bednarek I: MiR-424-3p suppresses galectin-3 expression and sensitizes ovarian cancer cells to cisplatin. Arch Gynecol Obstet 299: 1077-1087, 2019.
42. Geretto M, Pulliero A, Rosano C, Zhabayeva D, Bersimbaev R and Izzotti A: Resistance to cancer chemotherapeutic drugs is determined by pivotal microRNA regulators. Am J Cancer Res 7: 1350-1371, 2017.
43. Xu S, Tao Z, Hai B, Liang H, Shi Y, Wang T, Song W, Chen Y, OuYang J, Chen J, *et al*: miR-424(322) reverses chemoresistance via T-cell immune response activation by blocking the PD-L1 immune checkpoint. Nat Commun 7: 11406, 2016.
44. Song MK, Lee JH, Ryoo IG, Lee SH, Ku SK and Kwak MK: Bardoxolone ameliorates TGF-beta1-associated renal fibrosis through Nrf2/Smad7 elevation. Free Radic Biol Med 138: 33-42, 2019.
45. Tao Y, Sun C, Zhang T and Song Y: SMURF1 promotes the proliferation, migration and invasion of gastric cancer cells. Oncol Rep 38: 1806-1814, 2017.
46. Guo J, Xu G, Mao C and Wei R: Low expression of smurf1 enhances the chemosensitivity of human colorectal cancer to gemcitabine and cisplatin in patient-derived xenograft models. Transl Oncol 13: 100804, 2020.
47. Gozani O, Karuman P, Jones DR, Ivanov D, Cha J, Lugovskoy AA, Baird CL, Zhu H, Field SJ, Lessnick SL, *et al*: The PHD finger of the chromatin-associated protein ING2 functions as a nuclear phosphoinositide receptor. Cell 114: 99-111, 2003.